2005-09-01

Embedded slanted grating coupler for vertical coupling between fibers and silicon-on-insulator planar waveguides

Gregory P. Nordin
nordin@byu.edu

J. Jiang

B. Wang

Original Publication Citation

B. Wang, J. Jiang, and G. P. Nordin, "Embedded slanted grating coupler for vertical coupling between fibers and silicon-on-insulator planar waveguides," IEEE Phot. Techn. Lett. 17(9), pp. 1884-1886 (25)

Embedded Slanted Grating for Vertical Coupling Between Fibers and Silicon-on-Insulator Planar Waveguides

Bin Wang, *Student Member, IEEE*, Jianhua Jiang, and Gregory P. Nordin, *Member, IEEE*

***Abstract*—We propose a compact and efficient grating coupler for vertical coupling between optical fibers and planar waveguides. A grating with a parallelogram shape is designed to be etched through the entire high-index waveguide core. The coupler is optimized using a microgenetic algorithm coupled with a two-dimensional finite-difference time-domain method. Simulations show that up to 75.8% coupling efficiency can be obtained between a single-mode fiber and a 240-nm-thick silicon-on-insulator planar waveguide.**

***Index Terms*—Gratings, integrated optics, optical fiber coupling, waveguide components.**

I. Introduction

COMPACT and efficient slanted grating couplers (SLGCs) operating in the strong coupling regime have recently been proposed to vertically connect fibers and planar waveguides without intermediate optics [1]. This grating coupler utilizes a strong index modulated parallelogramic grating on top of a polymeric waveguide. Simulation results showed that it is possible to realize 66.8% coupling efficiency for a uniform SLGC and 80.1% for a fill-factor-varied nonuniform SLGC for a 20-μm grating length. We were originally motivated to examine such structures by the development of a new etching technique that readily achieves slanted etches [2]. Vertical fiber coupling allows for dense optical connection, and wafer-scale alignment and testing.

In this letter, we present a modified SLGC in which the slanted grating is completely embedded in the waveguide core. This embedded slanted grating coupler (ESGC) is especially well suited for high index contrast waveguides in which the core thickness is a few hundred nanometers. This permits the field distribution in the grating region of the ESGC to be centered within the waveguide, which improves the mode transition from the grating region to the nongrating region and thus reduces scattering loss at the boundary. We demonstrate the ESGC concept by applying it to a silicon-on-insulator slab waveguide.

Manuscript received February 4, 2005; revised April 7, 2005. This work was supported by the Defense Advanced Research Projects Agency under Grant N66001-01-8938 and by the National Science Foundation under Grant EPS-0091853.

The authors are with the Nano and Micro Devices Center, University of Alabama in Huntsville, Huntsville, AL 35899 USA (e-mail: wangb@email.uah.edu; jiangj@email.uah.edu; nordin@ece.uah.edu).

Digital Object Identifier 10.1109/LPT.2005.853236

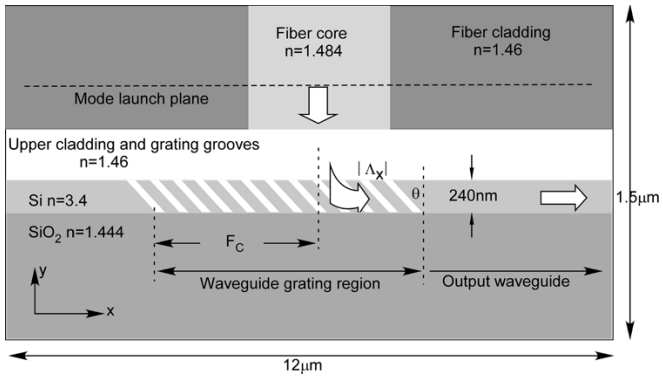

Fig. 1. Schematic diagram of ESGC geometry.

II. Structure and Simulation Method

Since an ESGC operates in the strong coupling regime, the effect of the grating cannot be treated as a small perturbation to the waveguide as in the analysis of conventional weakly modulated grating couplers. We have, therefore, applied the two-dimensional (2-D) finite-difference time-domain (FDTD) [3] method with Berenger's perfectly matched layer boundary conditions [4] to rigorously analyze and design ESGCs. Unless otherwise noted, all calculations are performed at $\lambda = 1.55$ μm.

Fig. 1 schematically illustrates the geometry of an ESGC. The grating is embedded in the waveguide core region with an overlying upper cladding that fills the grating grooves. The single-mode planar waveguide is a 240-nm-thick layer of Si with refractive index 3.4. The lower cladding of SiO_2 has refractive index of 1.444 and is assumed to be thick enough that no light is coupled into the Si substrate. The upper cladding is assumed to have a refractive index of 1.46.

The single-mode fiber has a core size of 4.4 μm. The core and cladding refractive indexes are 1.484 and 1.46, respectively. For 2-D analysis, the fiber is simulated as a planar waveguide. The entire structure fits in an overall FDTD simulation area of 12×1.5 μm. As shown in Fig. 1, the fundamental mode of the fiber waveguide is sourced at the top of the FDTD simulation region and propagates toward the grating coupler and is coupled into the waveguide traveling to the right. In order to save simulation time, we first use a coarse square Yee cell size of 10 nm. After a good solution is found, the Yee cell is decreased to 3 and 6 nm in the x and y directions, respectively, to fine tune and verify the coarse design. In all cases, we found excellent agreement between results run at the two grid sizes. Moreover, there was no observable effect for situations in which the

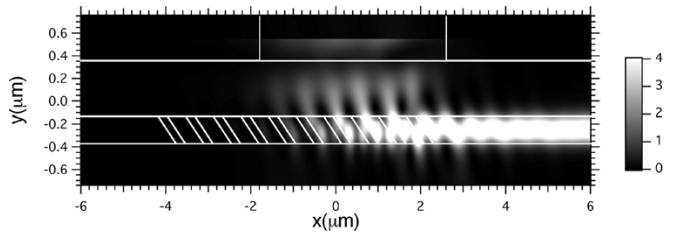

Fig. 2. Magnitude squared time averaged electric field as simulated by 2-D FDTD. Note that the vertical and horizontal dimensions are not drawn to scale.

grating geometrical parameters were not even multiples of the grid size. Transverse-electric polarized (electric field out of the plane) light is assumed. Further simulation shows that the coupling efficiency for transverse-magnetic polarization is very low (about -20 dB) for the structures described below.

To rapidly explore the device parameter space to find an efficient design, we apply the design tool reported in [5] which employs a parallel small population size genetic algorithm called micro-GA (μGA) as the global optimization method and 2-D FDTD as the rigorous electromagnetic computation engine. During μGA optimization, the independent variables are the grating period along the x direction (Λ_x), the fill factor (f, which is the ratio of the low index grating groove width and the period), the slant angle (θ) relative to waveguide normal, and the lateral distance F_c between the center of the fiber and the left edge of the bottom of the grating.

III. Result and Discussion

The magnitude squared time averaged electric field of one of the μGA optimized ESGCs is shown in Fig. 2 along with the ESGC geometry. The corresponding Λ_x, f, θ, and F_c are 0.6495 μm, 0.328 (the groove width is 213 nm), 59.71° and 4.28 μm, respectively. To determine the performance of the ESGC, we define the coupling efficiency as the ratio of the power carried by the mode of the waveguide to the incident power carried by fiber mode. A mode overlap integral calculation shows that the coupling efficiency for this optimized ESGC is 69.8%. Note that with a grating period of 0.6495 μm and ten periods, the grating spans less than 7 μm.

We now investigate the physical operation of the μGA optimized ESGC. First we investigate the phase-matching condition. For normal incidence, the well-known phase-matching condition for grating couplers can be expressed as [6]

$$n_{\text{eff}} = \frac{\lambda_0}{\Lambda_x}. \tag{1}$$

Equation (1) assumes $+1$ order operation of the ESGC, where n_{eff} is the effective index of a waveguide mode for which the phase match is satisfied. We substitute the optimized period $\Lambda_x = 0.6495$ μm and a wavelength of 1.55 μm into (1), and obtain $n_{\text{eff}} = 2.3864$. A simple mode calculation shows that the effective index of the fundamental mode of the output waveguide (without grating) is 2.834. Therefore, it is obvious that the phase match is not satisfied with respect to the fundamental mode of the output waveguide.

On the other hand, a rigorous leaky mode analysis [1] of the ESGC reveals that the grating region has a fundamental leaky mode with an effective index of 2.3972. Note this is very close to the n_{eff} required by the phase matching condition. The slight variation may be due to the fact that the incident fiber mode has a small angular spread (i.e., is not a plane wave) and that there are relatively few periods in the grating. Thus, we conclude that, in ESGC, the phase matching condition is satisfied with respect to the fundamental leaky mode in the grating region through the $+1$ diffraction order of the grating.

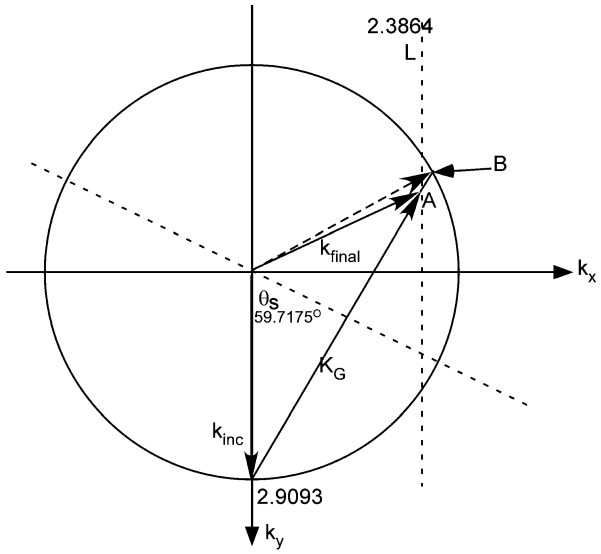

Fig. 3. K-vector diagram of ESGC.

Another important consideration in the design of grating couplers is Bragg diffraction, which can dramatically affect grating performance. Although it is well known that Bragg diffraction usually happens in relatively thick volume gratings, we find that the μGA optimized ESGC design operates near the Bragg diffraction condition [7], as shown below.

To study Bragg diffraction, we construct a k-vector diagram as shown in Fig. 3. Note that all k vectors in the figure are normalized by k_0, the free space k vector. The solid circle has a radius of 2.9093 and denotes the average refractive index of the grating layer (which is defined in [8]). The dotted slanted line refers to the orientation of the slanted grating ridges relative to the k_y axis, which is 59.71° in this case. The dotted vertical line, L at $k_x = 2.3864$ corresponds to the phase matching condition. $\vec{k}_{\text{inc}}$ is the normal incident k vector and $\vec{K}_G$ is the grating vector perpendicular to the orientation of the slanted ridges. The diffracted k vector, $\vec{k}_{\text{final}}$, which is the vectorial addition of $\vec{k}_{\text{inc}}$ and $\vec{K}_G$, should terminate on line L to satisfy the phase matching condition. From the diagram, we can see that $\vec{k}_{\text{final}}$ indeed terminates on line L at Point A. We also note that Point B, the intersection point of the extended grating vector and the solid circle, represents exactly Bragg diffraction. Point A is close to Point B, which means that the ESGC operates near the Bragg diffraction condition [7]. Bragg diffraction acts to suppress other diffraction orders and enforces unidirectional coupling in the ESGC.

The excitement of the fundamental leaky mode and the presence of Bragg diffraction should cause abnormal reflection and we should be able to identify the μGA optimized values on the reflection curve as discussed in [9]. To this end, we carried out a detailed rigorous coupled wave analysis (RCWA) [10] on the

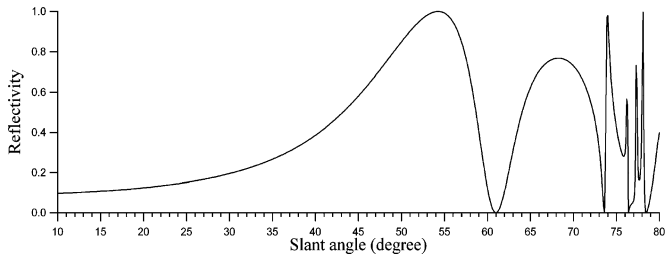

Fig. 4. Reflectivity of the optimized structure ESGC structure simulated by RCWA.

μGA optimized ESGC. Fig. 4 shows the diffraction efficiency of the zeroth reflected order as function of the slant angle. It is evident that the optimum slant angle 59.7° is very close to the minimum reflection angle of 61.5°. The small discrepancy is caused by the different source used in the RCWA (plane wave) and FDTD (waveguide mode) simulations. This provides an additional means to verify whether the ESGC design is optimal.

We now examine fabrication tolerances for the grating groove width and the slant angle for $\lambda = 1.55$ μm. The grating groove width can be difficult to control during fabrication and we find that a variation of ± 18 nm relative to the optimized value of 213 nm (or $\pm 8.45\%$ change) causes the coupling efficiency to drop to 62.2%. We also find that the coupling efficiency is greater than 63.1% for over a $\pm 3°$ change in the slant angle. We also simulated the performance of the structure as a function of the misalignment of the fiber position along the x direction. Results show that a misalignment within ± 0.7 μm is required for the coupling efficiency to be 63.5% or more.

To further improve the performance of ESGCs, we have also considered nonuniform fill factor [1] designs. In the μGA optimization of nonuniform ESGCs, the fill factors of all ten grating periods are varied independently within the range of 10% to 90%. The optimized ESGC parameters are: $\Lambda = 0.6573$ μm, $\theta = 60.35°$, and $F_c = 3.9$ μm. The coupling efficiency is improved to 75.8%. Fig. 5(a) shows the magnitude squared time averaged electric field and Fig. 5(b) shows the μGA optimized fill factor as a function of the ridge position in the x direction.

An important next step in evaluating the properties of ESGCs is to extend the 2-D results presented in this letter to a rigorous three-dimensional analysis. Currently, we are also investigating the fabrication feasibility of ESGCs.

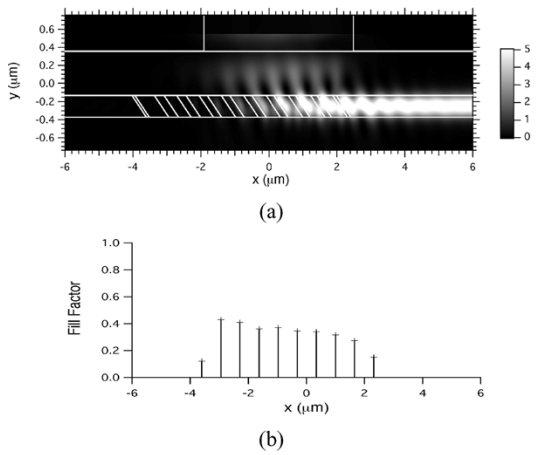

Fig. 5. (a) Image plot of the magnitude squared time averaged electric field simulated by 2-D FDTD. Note that the vertical and horizontal dimensions are not drawn to scale. (b) Fill factor distribution of the nonuniform ESGC in (a).

REFERENCES

[1] B. Wang, J. Jiang, and G. P. Nordin, "Compact slanted grating couplers," *Opt. Express*, vol. 12, pp. 3313–3326, Jul. 2004.
[2] M. Hoffbauer, private communication.
[3] A. Taflove, *Computational Electrodynamics: The Finite-Difference Time-Domain Method*. Norwood, MA: Artech House, 1995.
[4] J. P. Berenger, "A perfectly matched layer for the absorption of electromagnetic waves," *J. Comput. Phys.*, vol. 114, pp. 185–200, 1994.
[5] J. Jiang, J. Cai, G. P. Nordin, and L. Li, "Parallel micro-genetic algorithm design of photonic crystal and waveguide structures," *Opt. Lett.*, vol. 28, pp. 2381–2383, 2003.
[6] T. Tamir and S. T. Peng, "Analysis and design of grating couplers," *Appl. Phys.*, vol. 14, pp. 235–254, 1977.
[7] H. Kogelnik and T. P. Sosnowski, "Holographic thin film couplers," *Bell Syst. Tech. J.*, vol. 49, pp. 1602–1608, Sep. 1970.
[8] M. Li and S. J. Sheard, "Waveguide couplers using parallelogramic-shaped blazed gratings," *Opt. Commun.*, vol. 109, pp. 239–245, Jul. 1994.
[9] A. V. Tishchenko, N. M. Lyndin, S. M. Loktev, V. A. Sychugov, and B. A. Usievich, "Unidirectional waveguide grating coupling by means of parallelogramic grooves," *SPIE*, vol. 3099, pp. 269–277, 1997.
[10] M. G. Moharam and T. K. Gaylord, "Diffraction analysis of dielectric surface-relief gratings," *J. Opt. Soc. Amer.*, vol. 72, pp. 1385–1392, Oct. 1982.